for the structurally characterized complex *trans*-[MoOCl-(dppe)$_2$]Cl (ν(Mo=O) at 942 cm^{-1}).[24]

CV's of solutions of these complexes in 0.1 M TBAH/CH$_2$Cl$_2$ revealed the presence of a reversible one-electron reduction at $E_{1/2}$ = –1.17 V (X = Cl) and $E_{1/2}$ = –1.10 V (X = Br) and an irreversible oxidation at $E_{p,a}$ = +1.8 V (X = Cl) and +1.9 V (X = Br) vs Ag/AgCl. Irreversible processes associated with the oxidation of the outer-sphere halide ion are also seen (Table IV).

The ^{31}P{^{1}H} NMR spectra of these complexes recorded in CD$_2$Cl$_2$ exhibit a singlet at δ +48.8 (X = Cl) and δ +47.6 (X = Br). These chemical shifts are characteristic of five-membered rings formed by chelating phosphines.[25] The ^{1}H NMR spectra of [MoOX(dppbe)$_2$]X·nH$_2$O (X = Cl, Br) recorded in CD$_2$Cl$_2$ showed the expected phenyl ring resonances between δ +8.8 and +6.5. These spectra are almost identical with one another.

The low-frequency IR spectrum (Nujol mull) for [MoOCl-(dppbe)$_2$]Cl·3H$_2$O exhibits a strong absorption at 293 cm^{-1}, which is probably due to the ν(MoCl) mode. A similar band (at ~290 cm^{-1}) is seen the spectrum of the analogous PF$_6^-$ salt.

D. Consideration of Reactivities. In view of previous observations concerning the occurrence of chelating (α) and bridging (β) isomers for Mo$_2$X$_4$(LL)$_2$ compounds, the lack of evidence for the bridging form when LL = dppbe was unexpected. The recovery of the α-Mo$_2$X$_4$(dppbe)$_2$ species from methanol after brief reactions suggests that these isomers result from a kinetically favored pathway, behavior typical of other α-Mo$_2$X$_4$(LL)$_2$ complexes formed in this solvent.[4,5] In addition, the conversion of these products to the mononuclear compounds *trans*-MoX$_2$(dppbe)$_2$ further substantiates kinetic reaction control for dinuclear complex formation. Isolation of *trans*-MoX$_2$(dppbe)$_2$ as the major products from both [Mo$_2$X$_8$]$^{4-}$ and α-Mo$_2$X$_4$(dppbe)$_2$ reactants in the higher

boiling 1-propanol solvent indicates greater thermodynamic stability for these mononuclear complexes. Thus, the principal question regarding the observed reactivities involves the ready breakage of the metal–metal quadruple bond in preference to α → β isomerization. Interestingly, while the formation of *trans*-MoBr$_2$(dppe)$_2$ does accompany the rearrangement reaction of α-Mo$_2$Br$_4$(dppe)$_2$ to its β isomer, this mononuclear species is formed as a *minor* side product only.[6]

We are unable to say at present whether the bridging (β) dppbe isomer cannot be generated because of the inability of this ligand to bridge two metal centers in this type of complex or whether this form is accessible through an alternative synthetic route. However, we note that in the case of the analogous dirhenium(II) systems only the α isomers have been isolated, the β forms having defied our attempts to prepare them.[13]

The isolation and characterization of the mononuclear oxo species [MoOX(dppbe)$_2$]X·nH$_2$O from the reactions of octa-halodimolybdate(II) anions with dppbe in refluxing 1-propanol marks the first time that oxo–molybdenum(IV) species have been isolated from reactions of this type. Whether the oxygen is derived from 1-propanol or from adventitious water has not been established.

Supplementary Material Available: Tables of bond distances, bond angles, and thermal displacement parameters (4 pages); a list of observed and calculated structure factors (20 pages). Ordering information is given on any current masthead page.

(24) Bishop, M. W.; Chatt, J.; Dilworth, J. R.; Hursthouse, M. B.; Motevalli, M. *J. Chem. Soc., Dalton Trans.* **1979**, 1603.

(25) Garrou, P. E. *Chem. Rev.* **1981**, *81*, 229.

Contribution from the Anorganisch Chemisch Laboratorium, J. H. van't Hoff Instituut, University of Amsterdam, Nieuwe Achtergracht 166, 1018 WV Amsterdam, The Netherlands, and Institut für Anorganische Chemie der Universität München, Meiserstrasse 1, 8000 Munich 2, FRG

Bonding Mode Variations in Palladium(II) and Platinum(II) Azaphosphole Complexes: Identification by ^{1}H, ^{31}P, and ^{195}Pt NMR of N- and P-Coordination, Pt–Cl Addition to P, and Dimerization

Johanna G. Kraaijkamp,[1a] David M. Grove,[1a,b] Gerard van Koten,*[1a,b] and Alfred Schmidpeter[1c]

Received January 13, 1988

The 1,2,3-diazaphosphole P̄=C(H)C(Me)=NNMe (L$_A$) and the 1,2,4,3-triazaphospholes P̄=NC(Ph)=NNMe (L$_B$) and P̄=NN(Me)C(Me)=N (L$_C$) react with the halo-bridged dimers [MX$_2$(PEt$_3$)]$_2$ (M = Pt^{II}, Pd^{II}) to afford a variety of products with MX$_2$(PEt$_3$)L (L = di- or triazaphosphole) stoichiometry. With [PdCl$_2$(PEt$_3$)]$_2$ these azaphospholes produce *trans*-[PdCl$_2$(PEt$_3$)L] with σ-N-bonded L. From [PtBr$_2$(PEt$_3$)]$_2$ is obtained [PtBr$_2$(PEt$_3$)L] as a mixture of the cis σ-P coordination isomer with lesser amounts of the trans σ-N isomer. These azaphospholes all afford different products with [PtCl$_2$(PEt$_3$)]$_2$; the diazaphosphole L$_A$ produces mononuclear *cis*-[PtCl$_2$(PEt$_3$)L$_A$] (σ-P bound) whereas the triazaphospholes L$_B$ and L$_C$ produce dinuclear species that have symmetric and asymmetric structures, respectively. The new air-sensitive complexes have been principally characterized by a combination of ^{1}H, ^{31}P, and ^{195}Pt NMR solution spectroscopy.

Introduction

The azaphospholes[2] are heteroatomic aromatic ring systems which contain a two-coordinate trivalent phosphorus atom that is doubly bonded to carbon or nitrogen. Normally, i.e. in the acyclic nonconjugated case, such bonds readily undergo addition reactions, but in azaphospholes these bonds are stabilized by the cyclic delocalization. Complex formation can modify the tendency of an azaphosphole to give additions[2–4] to the various bonds depending on the coordination mode present.

The 1,2,3-diazaphosphole L$_A$ and the 1,2,4,3-triazaphospholes L$_B$ and L$_C$ (see Figure 1) have a variety of potential ligating sites available, of which the lone pair of phosphorus is common to all

(1) (a) University of Amsterdam. (b) Present address: Laboratory of Organic Chemistry, Department of Metal-Mediated Synthesis, University of Utrecht, Padualaan 8, 3584 CH Utrecht, The Netherlands. (c) Universität München.

(2) Schmidpeter, A.; Karaghiosoff, K. *Nachr. Chem., Tech. Lab.* **1985**, *33*, 793–799.

(3) Schmidpeter, A.; Tautz, H.; von Seyerl, J.; Huttner, G. *Angew. Chem.* **1981**, *93*, 420; *Angew. Chem., Int. Ed. Engl.* **1981**, *20*, 408.

(4) Kraaijkamp, J. G.; Ernsting, J.-M.; Grove, D. M.; van Koten, G.; Schmidpeter, A., manuscript in preparation.

---

* To whom correspondence should be addressed.

Table I. Analytical and IR[a] Data for Complexes **1, 3, 10,** and **12**

| compd | anal., % | | | | | IR ν(M–Cl), cm^{-1} |
	C	H	N	P	Cl	
trans-[PdCl$_2$(PEt$_3$)L$_A$] (**1**) found	29.74	5.64	6.74	14.40	17.22	349
calcd	29.32	5.41	6.84	15.13	17.31	
trans-[PdCl$_2$(PEt$_3$)L$_C$] (**3**) found	27.00	5.47	10.09	14.11	17.25	347
calcd	26.33	5.16	10.23	15.09	17.27	
cis-[PtCl$_2$(PEt$_3$)L$_A$] (**10**) found	24.55	4.60	5.57	*b*	14.30	319, 382
calcd	24.11	4.45	5.62		14.23	
[Pt$_2$Cl$_3$(PEt$_3$)$_2$(μ-L$_C$L$_C$Cl)] (**12**) found	21.53	4.50	8.24	12.30	14.45	*b*
calcd	21.66	4.24	8.42	12.41	14.20	

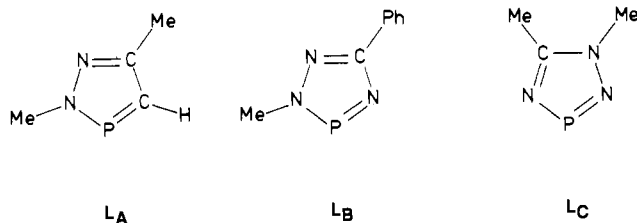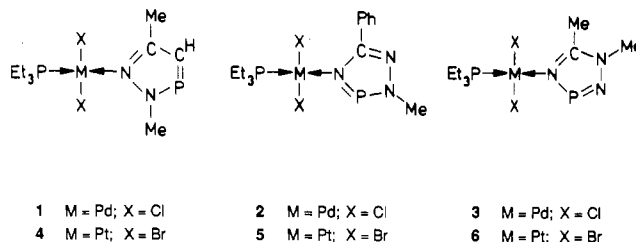[a]Nujol mull between CsI plates. [b]Not measured.

Figure 1. Azaphospholes L$_A$, L$_B$, and L$_C$.

1 M = Pd; X = Cl	**2** M = Pd; X = Cl	**3** M = Pd; X = Cl
4 M = Pt; X = Br	**5** M = Pt; X = Br	**6** M = Pt; X = Br

Figure 2. Schematic structures of **1–3** and **4–6**.

three. In addition to this, L$_A$ has a single σ-N-bonding site (–N=C) whereas L$_B$ and L$_C$ both have two such sites (–N=C and –N=P). Previous studies have shown that these azaphospholes coordinate exclusively with the phosphorus lone pair in carbonyl complexes in chromium,[3,5,6] molybdenum,[6] tungsten,[3,6] iron,[6] and manganese,[6] whereas in [Au^{III}Me$_2$Cl(L)] (L = di- and triazaphosphole) both σ-P (L$_B$) and σ-N (L$_A$ and L$_C$) modes are found.[7] Although it was anticipated that the azaphospholes L$_A$ and L$_C$ might be able to π-bond to Pt(0) substrates (i.e. η^2-P=N or η^2-P=C bonding), both ligands showed only the σ-P coordination mode in the complexes [Pt(PPh$_3$)$_n$L$_{4-n}$] (n = 2, 3).[8]

The present paper presents results concerning the products obtained from the interaction of L$_A$, L$_B$, and L$_C$ with halo-bridged Pt(II) and Pd(II) dimers. A forthcoming paper[4] is concerned with the reaction of these air-sensitive products with protic solvents such as MeOH. Some preliminary findings from both of these studies have been the subject of a communication.[9]

Experimental Section

All preparations were carried out under oxygen-free dry nitrogen with use of carefully dried and distilled solvents. The dimers [MX$_2$(PEt$_3$)]$_2$ (M = Pt, X = Cl, Br; M = Pd, X = Cl)[10] and the azaphospholes L$_A$,[11a,b] L$_B$,[11a,b] and L$_C$[11c] were prepared by literature methods.

The ^{1}H NMR spectra were recorded on Bruker WM-250 and Varian T-60 spectrometers. The ^{31}P{^{1}H} NMR spectra were recorded on Bruker WP-80 (32.4 MHz) and Varian XL-100 (40.5 MHz) spectrometers with chemical shifts referenced to external H$_3$PO$_4$ (0.0 ppm) and with a positive value indicating a shift to lower field. The ^{195}Pt{^{1}H} NMR spectra were recorded at ca. 53.5 MHz on a Bruker WM-250 spectrometer, on which the TMS ^{1}H resonance of a CDCl$_3$ solution is 250 132 847 Hz. The measured absolute frequency of a ^{195}Pt resonance was converted (making allowance for the various deuterium lock signals) to a standard frequency (TMS ^{1}H resonance at 100 MHz).[12] Chemical shifts are

reported relative to 21.4 MHz with a positive value being to higher frequency (cf. PtCl$_6^{2-}$: 21 496 770 Hz, +4522 ppm).[13]

The ^{195}Pt shifts (Table III) were calculated from the following measured ^{195}Pt resonance positions (Hz): 53 523 252 (**7**); 53 520 868 (**8**); 53 540 024 (**10**); 53 557 280 (**11**); 53 541 844 [Pt$_1$] and 53 540 105 [Pt$_2$] (**12**).

Conductivity measurements under a nitrogen atmosphere were carried out on ca. 1 × 10^{-2} M solutions of **11** and **12** in CH$_2$Cl$_2$ by using a Philips PR 9512/00 microcell with a Consort K720 conductometer. For comparative purposes [Pt$_2$(PBu$_3$)$_4$Cl$_2$]$^{2+}$(BF$_4^-$)$_2$, NBu$_4^+$Br$^-$, *cis*-[Pt(PBu$_3$)$_2$Cl$_2$], and [Pt$_2$(PEt$_3$)$_2$Cl$_4$] gave molar conductivity values, Λ_M, of 9.9, 4.0, 0.42, and 0.02 cm^2 Ω^{-1} mol^{-1}, respectively.

IR spectra were recorded as Nujol mulls on a Perkin-Elmer 283 spectrometer.

Elemental analyses were carried out by the Elemental Analytical Section of the Institute for Applied Chemistry, TNO, Zeist, The Netherlands.

Preparation of the Azaphosphole Complexes 1–12. To stirred, powdered [MX$_2$(PEt$_3$)]$_2$ (0.5 mmol) was added a solution of the azaphosphole L (1.03 mmol) in CH$_2$Cl$_2$ (2 mL) at room temperature. After a few minutes a clear solution was obtained, and after the solution stood for 24 h, the solvent was removed in vacuo. The solid yellow residue was washed with pentane (2 × 5 mL) and dried in vacuo to afford the air-sensitive products in typically 80–90% yield. Purity, as estimated by ^{31}P NMR, was usually greater than 95%.

Results

Reaction of the azaphosphole ligands L$_A$, L$_B$, and L$_C$ with the halo-bridged dimers [MX$_2$(PEt$_3$)]$_2$ (M = Pt, X = Cl, Br; M = Pd, X = Cl) in 2:1 molar ratio affords a variety of solid, yellow, air-sensitive products, **1–12**, which all have a MX$_2$(PEt$_3$)L (L = di- or triazaphosphole) stoichiometry. These products have low solubility in hexane and toluene but are readily soluble in dichloromethane and chloroform. With protic solvents they react to form unusual products, whose characterization by spectroscopic methods and X-ray diffraction studies is the central theme of a forthcoming paper.[4] Elemental analysis proved to be experimentally demanding, and since the data obtained for a few representative species (Table I) only served to confirm the known reaction stoichiometry, its use was not pursued for all complexes. Characterization of the overall metal geometry and the azaphosphole coordination mode(s) in **1–12**, shown schematically in Figures 2, 4 and 5, was determined principally by IR and solution NMR spectroscopy. The IR ν(M–X) data are included in Table

(5) Issleib, R.; Vollmer, G.-R. *Z. Anorg. Allg. Chem.* **1981**, *481*, 22–32.
(6) Weinmaier, J. H.; Tautz, H.; Schmidpeter, A.; Pohl, S. *J. Organomet. Chem.* **1980**, *185*, 53–68.
(7) Dash, K. C.; Schmidbaur, H.; Schmidpeter, A. *Inorg. Chim. Acta* **1980**, *41*, 167–170.
(8) Kraaijkamp, J. G.; van Koten, G.; Vrieze, K.; Grove, D. M.; Klop, E. A.; Spek, A. L.; Schmidpeter, A. *J. Organomet. Chem.* **1983**, *256*, 375–389.
(9) Kraaijkamp, J. G.; van Koten, G.; Vrieze, K.; Grove, D. M.; Abbel, G.; Stam, C. H.; Schmidpeter, A. *Inorg. Chim. Acta* **1984**, *85*, L33–L34.
(10) Hartley, F. R. *Organomet. Chem. Rev.* **1970**, *A6*, 119–137.
(11) (a) Weinmaier, J. H.; Brunnhuber, G.; Schmidpeter, A. *Chem. Ber.* **1980**, *113*, 2278–2290. (b) Luber, J.; Schmidpeter, A. *Angew. Chem.* **1976**, *88*, 91–92; *Angew. Chem., Int. Ed. Engl.* **1976**, *15*, 111–112. (c) Schmidpeter, A.; Luber, J.; Tautz, H. *Angew. Chem.* **1977**, *89*, 554–555; *Angew. Chem., Int. Ed. Engl.* **1977**, *16*, 546–547.

(12) (a) McFarlane, W. *Proc. R. Soc. London, Ser. A* **1968**, *306*, 185–199. (b) Harris, R. K.; Kimber, B. J. *J. Magn. Reson.* **1975**, *17*, 174–188.
(13) Kidd, R. G.; Goodfellow, R. G. In *NMR and the Periodic Table*; Harris, R. K., Mann, B. E., Eds.; Academic: London, New York, San Francisco, 1978.

Table II. ^{1}H NMR Data for Azaphospholes L_A, L_B, and L_C and Their Pt(II) and Pd(II) Complexes **1–12**^{a}

compd	donor	L δ(HC=P)	δ(MeN)	δ(MeC)	PEt$_3$ δ(CH$_2$)^b	δ(CH$_3$)^b
L_A		7.25 [43.7]	3.66 [7.6]	2.33 [1.3]		
cis-[PtCl$_2$(PEt$_3$)L$_A$] (**10**)	P	6.90 [46]	4.01 [10]	2.43 [1]	2.0	1.2
cis-[PtBr$_2$(PEt$_3$)L$_A$] (**7**)	P	6.92 [46]	4.02 [10]	2.48 [1]	2.0	1.1
trans-[PtBr$_2$(PEt$_3$)L$_A$] (**4**)	N	*c*	4.38 [10]	2.85 [2]	2.0	1.1
trans-[PdCl$_2$(PEt$_3$)L$_A$] (**1**)	N	7.56 [44]	4.50 [7]	2.85 [*d*]	2.0	1.3
L_B			3.97 [6.2]			
cis-[PtBr$_2$(PEt$_3$)L$_B$] (**8**)	P		4.25 [10]		2.2	1.3
trans-[PtBr$_2$(PEt$_3$)L$_B$] (**5**)	N		4.22 [8]		2.2	1.3
trans-[PdCl$_2$(PEt$_3$)L$_B$] (**2**)	N		4.17 [8]		2.1	1.4
[PtCl(PEt$_3$)$_2$(μ-L$_B$Cl)]$_2$ (**11**)	P, N^e		2.60 [15]		2.0	1.0
L_C			4.07 [1.4]	2.65 [0.7]		
cis-[PtBr$_2$(PEt$_3$)L$_C$] (**9**)^e	P		4.07 [*d*]	2.70 [*d*]	2.2	1.2
trans-[PtBr$_2$(PEt$_3$)L$_C$] (**6**)	N		4.07 [*d*]	2.94 [*d*]	2.2	1.2
trans-[PdCl$_2$(PEt$_3$)L$_C$] (**3**)	N		4.05 [*d*]	3.00 [*d*]	2.0	1.3
[Pt$_2$Cl$_3$(PEt$_3$)$_2$(μ-L$_C$L$_C$Cl)] (**12**)	*e*		3.88 [*d*]	2.40 [*d*]	2.3	1.1
			3.70 [*d*]	2.22 [*d*]	2.3	1.1

^{a} Spectra were recorded in CDCl$_3$ at room temperature; δ is relative to TMS with coupling constants ${}^nJ({}^{31}P,{}^1H)$ (in brackets) given in Hz. Data for the pairs **4** and **7**, **5** and **8**, and **6** and **9** are from the two-component mixtures. The Ph signals of L$_B$ were found in the range 7.2–8.5 ppm. ^{b} Complex multiplet. ^{c} Obscured by more intense signals of **7**. ^{d} Not resolved. ^{e} See text.

I, and NMR data are collected in Table II (^{1}H) and Table III (^{31}P{^{1}H} and ^{195}Pt{^{1}H}). Except for dimeric **11**, where there still remains some uncertainty concerning its proposed structure, all complexes could be unambiguously identified by these characteristic data.

In these Pt(II) and Pd(II) complexes various metal geometries with both σ-P and σ-N coordination modes of the azaphosphole are realized. Not only in the N-coordinated complexes **1–6** but also in the P-coordinated complexes **7–10** it is assumed that the metal center lies in the same plane as the azaphosphole ring. This means a trigonal-planar surrounding of phosphorus as was established in [CrL$_C$(CO)$_5$] by X-ray analysis.^{6}

For clarity of presentation, the σ-monodentate-bonded azaphosphole rings in Figures 2 and 4 are shown coplanar with the metal coordination plane. Depending on the steric hindrance encountered, the planar azaphosphole ligands will, in fact, either be free to rotate about the donor atom to metal bond or be restricted to a wagging motion so that the averaged position is approximately perpendicular to the metal coordination plane; the present data do not discriminate between these possibilities.

In the following sections the principal evidence used for the identification of particular products is described, with trends and their significance being discussed later.

i. Reaction of L with [PdCl$_2$(PEt$_3$)]$_2$. The 2:1 reaction of the azaphospholes L$_A$, L$_B$, and L$_C$ with this chloro-bridged dimer affords only *trans*-[PdCl$_2$(PEt$_3$)L] complexes **1–3** (figure 2), which in all cases have σ-N-bonded L. This bonding mode can be inferred from the ^{31}P NMR data. First, a coupling between the azaphosphole phosphorus, P$_L$, and P$_E$ (the phosphorus donor of PEt$_3$), which is anticipated for either a cis or a trans arrangement of two σ-P donors on Pd, is not observed. Second, the phosphorus coordination chemical shift, $\Delta\delta$ [δ(P)$_{complex}$ – δ(P)$_{ligand}$], of P$_L$ is quite small (ca. ±10 ppm) compared to the $\Delta\delta$ values found for azaphospholes σ-P-bound to Pt(0) (ca. –35 ppm)^9 and Pt(II) (ca. –60 ppm) (vide infra); δ(P) values for the free ligands L$_A$, L$_B$, and L$_C$ (in CDCl$_3$) are 228.9, 253.3, and 257.1 ppm, respectively. Finally, the significantly downfield chemical shift of P$_E$ (36.5 ± 1 ppm) suggests a trans N–Pd–P$_E$ arrangement (cf. *trans*-[PdCl$_2$(PEt$_2$Ph)(py)], δ(P) = 27.3; py = pyridine),^{14} which for **1–3** finds further support from the single IR ν(M–Cl) value of ca. 350 cm^{-1}.

The ^{1}H NMR spectra also present a consistent picture of σ-N azaphosphole coordination in complexes **1–3** and at the same time allow discrimination of N(=C) or N(=P) bonding in **2** and **3**. In **1**, where L$_A$ has only one σ-N-bonding mode possible, both diazaphosphole Me substituents are brought close to the metal
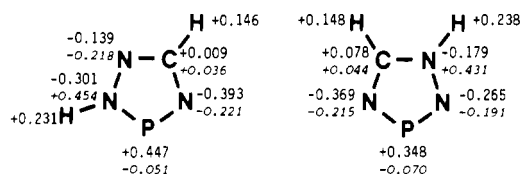
Figure 3. Distribution of total charges, with π-charges in italics, in the model compounds L$_B'$ and L$_C'$ (1,2,4,3-2H- and 1,2,4,3-1H-triazaphosphole, respectively) as calculated by MNDO.

7 X = Br
10 X = Cl
8
9
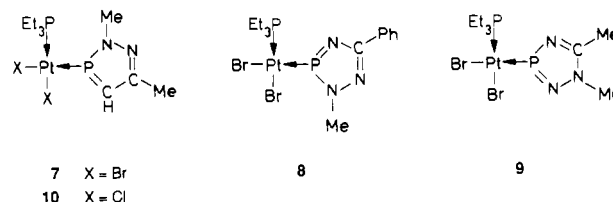
Figure 4. Schematic structures of **7–10**.

center and this is reflected in the significant downfield shifts of their ^{1}H NMR resonances (see Table II). For **2**, σ-N(=P) coordination is indicated by the NMe group ^{1}H NMR shift, which is similar to that of free L$_B$; σ-N(=C) coordination can be seen to be sterically less favorable. In the case of **3** there is a small downfield shift of the CMe ^{1}H resonance, which, when examined with data from complexes such as [Au^{III}Me$_2$Cl(L$_C$)],^{7} is consistent with N(=C) rather than N(=P) coordination.

Since the N(=C) and N(=P) coordination modes in **2** and **3**, respectively (as well as in **5** and **6**; vide infra), both involve the N-4 atom in a delocalized system, then they should be considered as being similar rather than different. This proposal is in agreement with MNDO-calculated charge distributions in the 1,2,4,3-2H- and 1,2,4,3-1H-triazaphospholes L$_B'$ and L$_C'$ (L$_B$ and L$_C$ with H instead of organic substituents; see Figure 3) which indicate that of the ring nitrogen atoms it is always N-4, i.e. N(=P) in L$_B'$ and N(=C) in L$_C'$, that carries the highest negative charge.

ii. Reaction of L with [PtBr$_2$(PEt$_3$)]$_2$. The 2:1 reaction of the azaphospholes L$_A$, L$_B$, and L$_C$ with this bromo-bridged Pt dimer yields a simple two-component mixture of the mononuclear product *trans*-[PtBr$_2$(PEt$_3$)L], in which L is σ-N bound (**4–6**), and *cis*-[PtBr$_2$(PEt$_3$)L] (**7–9**), in which L is σ-P bound (Figure 4). P-coordination always predominates; the ratio of P- to N-coordinated isomers for L$_A$, L$_B$, and L$_C$ is approximately 2:1 (**7:4**), 2:1 (**8:5**), and 4:1 (**9:6**), respectively, as judged from ^{31}P NMR signal intensities. The individual complexes have not been separated, and all solution NMR data relate to the two-component systems. Limiting ^{31}P NMR data for complexes **8** and **9** were

(14) Balimann, G.; Pregosin, P. S. *J. Magn. Reson.* **1976**, *22*, 235–241. δ(P) was extracted from Figure 2 of this reference.

Table III. ^{31}P and ^{195}Pt NMR Data for Complexes 1–12[a]

compd	L donor	P_L			P_E			
		$\delta(P)$	$^nJ(Pt,P)$[b]	$\Delta\delta$[c]	$\delta(P)$	$^1J(Pt,P)$	$^2J(P_E,P_L)$	$\delta(Pt)$[d]
trans-[PdCl$_2$(PEt$_3$)L$_A$] (1)	σ-N	236.5		+7.6	36.2			
trans-[PdCl$_2$(PEt$_3$)L$_B$] (2)	σ-N	244.8		−8.5	37.3			
trans-[PdCl$_2$(PEt$_3$)L$_C$] (3)	σ-N	245.9		−11.2	35.6			
trans-[PtBr$_2$(PEt$_3$)L$_A$] (4)	σ-N	234.9	<5	+6.0	−2.3	3426		
trans-[PtBr$_2$(PEt$_3$)L$_B$] (5)	σ-N	241.5	115[e]	−11.8	0.9	3447		
trans-[PtBr$_2$(PEt$_3$)L$_B$] (5)[f]	σ-N	239.3	117[e]	−14.0	−1.3	3370		
trans-[PtBr$_2$(PEt$_3$)L$_C$] (6)	σ-N	244.6	91[e]	−12.5	−2.5	3384		
trans-[PtBr$_2$(PEt$_3$)L$_C$] (6)[f]	σ-N	241.9	93[e]	−15.2	−3.0	3311		
cis-[PtBr$_2$(PEt$_3$)L$_A$] (7)	σ-P	162.6	4528	−66.3	15.2	2963	16	−97
cis-[PtBr$_2$(PEt$_3$)L$_B$] (8)	σ-P	190.7	5155	−62.6	18.7	2841	16	−140
cis-[PtBr$_2$(PEt$_3$)L$_B$] (8)[f]	σ-P	190.0	5298	−63.3	19.5	2795	18	
cis-[PtBr$_2$(PEt$_3$)L$_C$] (9)	σ-P	~211	g	~−46	16.6	2960	25	
cis-[PtBr$_2$(PEt$_3$)L$_C$] (9)[f]	σ-P	204.5	5301	−52.6	17.5	2872	20	
cis-[PtCl$_2$(PEt$_3$)L$_A$] (10)	σ-P	166.1	4676	−62.8	16.8	2960	25	+217
[PtCl(PEt$_3$)$_2$(μ-L$_B$Cl)]$_2$ (11)	σ-P, σ-N	65.2	5728, 124[e]	−188.1	10.6	3250	24	+539
[Pt$_2$Cl$_3$(PEt$_3$)$_2$(μ-L$_C$L$_C$Cl)] (12)	σ-P	109.8[h]	5970, 88[i]	−152.3	10.9[h]	3135	23	+251 [Pt$_1$]
	σ-P, σ-N	93.1[j]	5220, 20[i]	−164.0	14.3[j]	3472	18	+218 [Pt$_2$]
cis-[PtCl$_2$(PEt$_3$)$_2$][k]					8.7	3560		+47

[a] In CDCl$_3$ at room temperature unless otherwise stated. J values are in Hz; $\delta(^{31}P)$ is relative to external H$_3$PO$_4$ (85%), and $\delta(^{195}Pt)$ is relative to 21.4 MHz (see Experimental Section). Complexes 4 and 7, 5 and 8, and 6 and 9 were measured as the two-component mixtures. [b] $n = 1$ unless otherwise stated. [c] Coordination chemical shift as defined in ref 13. [d] See Experimental Section for measured resonance frequency. [e] $n = 2$. [f] CD$_2$Cl$_2$ at −40 °C. [g] Too broad for accurate determination. [h] P$_1$ σ-P-bound to Pt$_1$. [i] $n = |2+3|$. [j] P$_2$ σ-P-bound to Pt$_2$; $^3J(P_{2L},P_{1E}) = 3.5$ Hz, $^3J(P_{1L},P_{2L}) = 13.5$ Hz. [k] Data from ref 18.

obtained at −40 °C; at room temperature the P$_E$ signals were sharp while the P$_L$ signals were broadened. This is most likely due to a temperature-dependent relaxation enhancement of P$_L$ afforded by the two adjacent ^{14}N nuclei;[15] it does not necessarily indicate the onset of azaphosphole fluxionality.

For complexes 4–9 the presence of the ^{195}Pt isotope ($I = {}^1/_2$, 33.7% natural abundance) that can couple to both ^1H and ^{31}P provides more detailed data on the metal coordination sphere and the bonding modes of the ligands than was the case for the palladium species 1–3. For example, the σ-P coordination of P$_L$ in 7–9 follows directly from the observation of large $J(Pt,P_L)$ values (>4.5 kHz) and the cis arrangement of the phosphorus donors P$_L$ and P$_E$ is evident from the coupling $J(P_E,P_L)$ of ca. 15–20 Hz.[16] All other spectroscopic data (e.g. $\delta(P)$ and $\delta(H)$ values etc.; see Tables II and III) confirm these deductions. For the *trans*-[PtBr$_2$(PEt$_3$)L] σ-N-bound species 4–6 it is the absence of a large $J(Pt,P_L)$ value combined with the small coordination chemical shift of P$_L$ which indicates that the azaphospholes are not σ-P bound. The deduction of a trans N–Pt–P geometry is based on the value of $\delta(P_E)$ (ca. 0 ppm) that is consistent with PEt$_3$ being trans to a nitrogen donor ligand (cf. *trans*-[PtCl$_2$(PEt$_3$)(py)], $\delta(P_E)$ = 0.4 and $^1J(Pt,P_E)$ = 3362 Hz,[17] and *cis*-[PtCl$_2$(PEt$_3$)$_2$], $\delta(P_E)$ and 8.7 and $^1J(Pt,P_E)$ = 3560 Hz[18]). The comparability of ^1H NMR data for the azaphosphole Me substituents in the pairs 1 and 4, 2 and 5, and 3 and 6 clearly indicates that the palladium and platinum complexes for each azaphosphole are analogous with respect to the σ-N ligand coordination mode. Since ^{31}P chemical shifts are a composite from several sources,[16] there is no simple correlation between $\delta(P)$ values in corresponding Pt(II) and Pd(II) complexes. The rather large difference in $\delta(P_E)$ of ca. 38 ppm between the analogous *trans*-[PdCl$_2$(PEt$_3$)L] (1–3) and *trans*-[PtCl$_2$(PEt$_3$)L] (4–6) might at first sight seem unexpected but is consistent with the available data for [MX$_2$(PR$_3$)Y] (M = Pt, Pd; X = halide; Y = N-donor ligand) species (see Discussion).

iii. Reaction of L with [PtCl$_2$(PEt$_3$)]$_2$. The azaphospholes L$_A$, L$_B$, and L$_C$ reacted with [PtCl$_2$(PEt$_3$)]$_2$ in a 2:1 molar ratio to afford in each case a single product of PtCl$_2$(PEt$_3$)L stoichiometry.
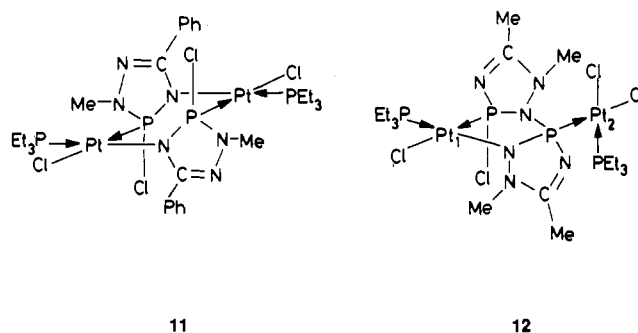

11 **12**

Figure 5. Schematic structures of dinuclear 11 and 12.
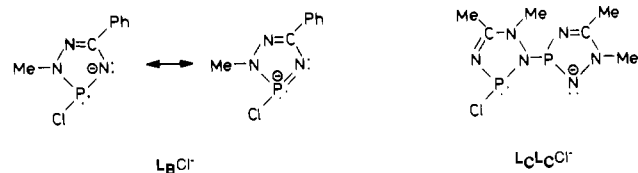
Figure 6. Anionic ligands L$_B$Cl and L$_C$L$_C$Cl.

However, the product is of a different structural type for each ligand. The product with L$_A$ is solely *cis*-[PtCl$_2$(PEt$_3$)L$_A$] (10) with a σ-P-bound diazaphosphole and with NMR parameters similar to those of *cis*-[PtBr$_2$(PEt$_3$)L$_A$] (7). In contrast, both L$_B$ and L$_C$, which contain a −P=N− function, form dinuclear Pt species containing modified triazaphosphole ligands that no longer have aromatic character.

With L$_B$ the platinum centers become bridged by two identical anionic (L$_B$Cl) units (see Figure 6) to form the symmetric dimer [PtCl(PEt$_3$)(μ-L$_B$Cl)]$_2$ (11). The tentatively postulated dinuclear structure (Figure 5) is based both on its molar conductivity of 0.25 cm^2 Ω^{-1} mol^{-1} (indicative of a nonionic formulation) and on its ^{31}P and ^{195}Pt NMR data. In the ^{31}P NMR spectrum there is one resonance pattern for both the P$_E$ and the P$_L$ signals; i.e., there is one PEt$_3$ and one triazaphosphole phosphorus atom environment. The $\delta(P_L)$ value is so high field that rehybridization at this center (from ψ-trigonal to ψ-tetrahedral) is likely to have occurred. Both signals show large $J(Pt,P)$ values associated with platinum bound to σ-P donors, and $J(P_E,P_L)$ is indicative of a *cis*-PtP$_E$P$_L$ fragment. More importantly, P$_L$ shows a distinctive long-range coupling to a second platinum center ($^nJ(Pt,P_L)$) = 124 Hz) and hence the azaphosphole is present as a bridging ligand. Furthermore, the ^{195}Pt spectrum of 11 shows a single eight-line

(15) Abragam, A. *The Principles of Nuclear Magnetism*; Clarendon: Oxford, England, 1961; p 309.

(16) Pregosin, P. S.; Kunz, R. W. In *NMR: Basic Principles and Progress*; Diehl, P., Fluck, E., Kosfeld, R., Eds.; Springer-Verlag: Berlin, Heidelberg, New York, 1978; vol. 16.

(17) Pidcock, P. D.; Jacobson, B.; Pidcock, A. *J. Chem. Soc., Dalton Trans.* **1977**, 2038–2042.

(18) Anderson, D. W. W.; Ebsworth, E. A. V.; Rankin, D. W. H. *J. Chem. Soc., Dalton Trans.* **1973**, 2370–2373.

pattern for only one type of platinum coupled to three separate phosphorus centers. The simplest molecule combining all these features is a symmetric dimer. Consequently, the ^{31}P and [195]Pt NMR spectrum of **11** can be satisfactorily described, and simulated, as a summation of an AA′BB′ (A = A′ = P_L; B = B′ = P_E) spin system without spin-active [195]Pt nuclei together with AA′BB′X and AA′BB′XX′ systems for isotopomers having one and two [195]Pt nuclei, respectively (the respective natural abundances being 44, 45, and 11%). The observed coupling patterns in these spectra do not, unfortunately, show any multiplicity or second-order effects that can be used to extract $J(A,A')$, $J(B,B')$, or $J(X,X')$. From a detailed analysis of chemical shift and coupling data from all the NMR spectra the most chemically reasonable structure of **11** shown in Figure 5 was deduced. However, it must be stressed that the available data are open to alternative interpretations, and in particular the δ(Pt) value of +539 ppm is not readily explained.

Molecular models of this proposed dimer show that a six-membered P̄t–P–N–Pt–P–N ring when adopting a chair conformation with the L_BCl rings oriented away from each other can produce a species with no obvious adverse steric interactions. A corresponding ring skeleton has been suggested for the compound $(\rightarrow$PtPh(PPh₃)NPhPPh₂$\rightarrow$)₂.[19] The rationale behind the formation of **11** is discussed later.

From the reaction of L_C with [PtCl₂(PEt₃)]₂ is obtained the single asymmetric dinuclear platinum species **12** having two different platinum coordination spheres and an unusual bridging system that has a P–N bond between the two, no longer aromatic, azaphosphole units (Figure 5). The first triazaphosphole unit forms a simple two-atom –P–N– bridge between a {PtCl(PEt₃)} ([Pt₁]) and a {PtCl₂(PEt₃)} ([Pt₂]) fragment. The second L_C unit, which (like L_B in **11**) has gained a Cl atom, σ-P-coordinates to platinum and forms a new N–P bond between itself and the phosphorus donor of the bridging L_C unit. This complex bridging ligand, which has been abbreviated as $L_C L_C$Cl (see Figure 6), has the azaphosphole phosphorus atoms involved in both a Pt–N–P–N–P ring and one other five-membered heteroatom ring. The basic elements of this proposed structure for **12** come from ^{31}P and [195]Pt NMR.

The most significant ^{31}P NMR spectral features are (a) two P_E and two P_L signals with J(Pt,P) and $J(P_E,P_L)$ values indicative of two different cis Pt$P_E P_L$ units, (b) P_L chemical shifts that are significantly high field, suggesting ψ-tetrahedral P_L geometries, (c) long-range couplings to a second platinum atom for both P_L signals (^nJ(Pt,P_L) = 88 and 20 Hz), indicating a dinuclear structure, and (d) a resolved coupling of 14 Hz between the two different P_L signals, which is strong evidence for a direct linkage between the two azaphosphole systems. The [195]Pt NMR spectrum of **12** (Figure 7) confirms the presence of two different platinum centers by exhibiting two sets of resonances, each of which is an eight-line pattern arising from coupling to three inequivalent phosphorus atoms; there is no observable ^nJ(Pt₁,Pt₂). Both ^{31}P and [195]Pt NMR spectra have been successfully simulated by using the data of Table III. In reflection of the molecular asymmetry of this complex, the ^{1}H NMR spectrum shows two *N*-Me and two *C*-Me azaphosphole substituent resonances that are shifted strongly downfield relative to the free ligand signals. Clearly, the azaphosphole ligands have been significantly changed upon coordination. However, the new local environments of the two rings are fairly similar since within the *C*-Me and *N*-Me pairs the chemical shift differences are not large.

If we bear in mind the above constraints and conclusions, together with the nonionic nature (measured molar conductivity, Λ_M, in CH₂Cl₂ at room temperature is 0.19 cm² Ω⁻¹ mol⁻¹) and the remaining spectral data, the asymmetric dimeric structure shown in Figure 5 is deduced as the most likely structure for **12**. There is no direct evidence regarding the relative orientation of
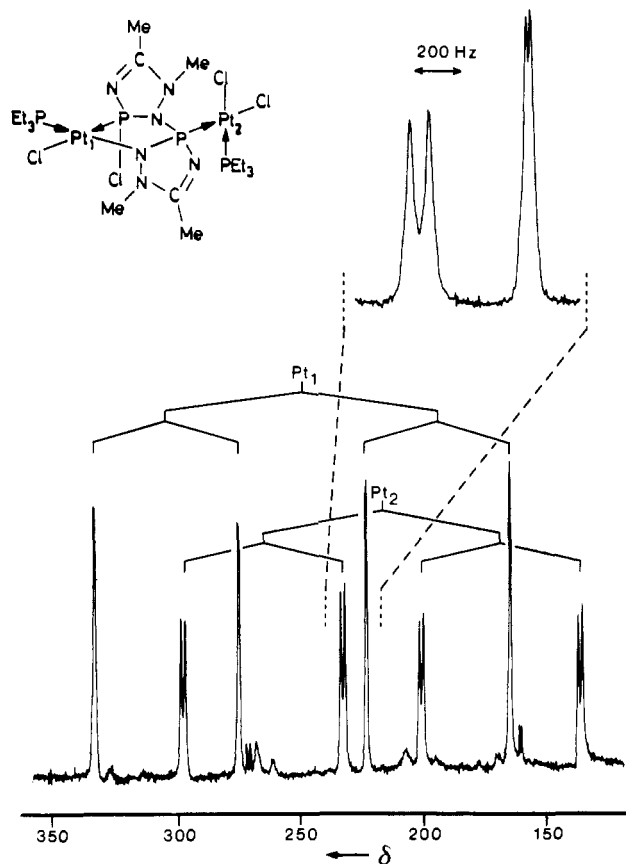

Figure 7. 53.5 MHz [195]Pt{^{1}H} NMR spectrum (CDCl₃) of dinuclear **12** with the ^1J(Pt,P) coupling scheme and an expansion of the central lines showing long-range ^nJ(Pt,P). Small nonassigned peaks are impurities.

the two P̄N̄N̄C=N rings in **12**, and this figure illustrates only one of several possible arrangements in which rotation about the P–Pt{Cl₂(PEt₃)} bond can provide the molecule with a fair degree of freedom in reducing steric interactions.

Discussion

Formation of 1–12. Normally the ring phosphorus of an azaphosphole does not protonate or alkylate since that would make it three-coordinate and thereby cause too much loss of cyclic resonance. The donor ability of an azaphosphole phosphorus atom only shows up in complex formation. Even the N-coordination can be preferred to P-coordination, as is the case for L_A, L_B, and L_C with the {PdCl₂(PEt₃)} unit. With the {PtBr₂(PEt₃)} unit, where these three azaphospholes form both N- and P-bonded complexes, there seems to be some preference for the phosphorus site. In these complexes N-coordination is associated with a trans halogen atom arrangement and P-coordination with a cis arrangement, geometries that are consistent with the known behavior of such Pt(II) and Pd(II) fragments with weak σ-donors.[20]

The {PtCl₂(PEt₃)} unit clearly coordinates preferentially to phosphorus, and with the diazaphosphole L_A, which has no pyridinic nitrogen adjacent to phosphorus, the formation of mononuclear *cis*-[PtCl₂(PEt₃)L_A] (**10**) is preferred. The dinuclear species **11** and **12**, formed by L_B and L_C, respectively, can be plausibly derived from the corresponding P-coordinated analogues of **10**. In these postulated primary complexes, azaphosphole P-coordination will increase the acceptor quality of the phosphorus and then ease addition to the double bond in which it is involved. Therefore, a reasonable initial step toward dimerization (see Figure 8) is a chloride shift from platinum to phosphorus that can be seen as an oxidative addition of Pt–Cl to phosphorus. Such a chloride shift will be assisted if, at the same time, there is attack on platinum by the N(=P) donor of a second molecule of primary

---

(19) Beck, W. In *Transition Metal Chemisry*; Müller, A., Diemann, E., Eds.; Verlag Chemie: Weinheim, West Germany, 1981; p 307. However, the structure has not been definitely established: Beck, W., personal communication.

(20) Hartley, F. R. *The Chemistry of Platinum and Palladium*; Applied Science Publishers: London, 1973.
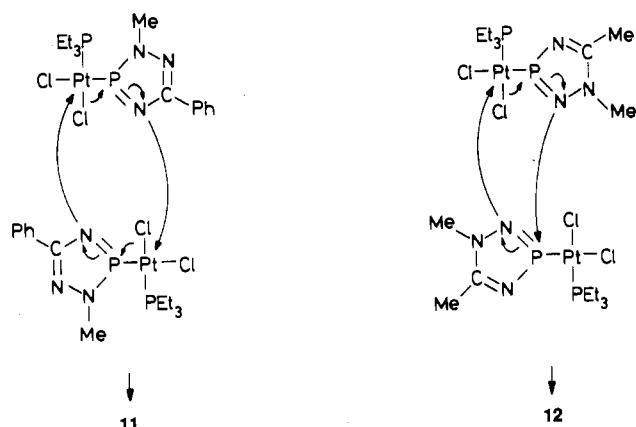
Figure 8. Proposed mechanisms leading from mononuclear σ-P-coordinated *cis*-[PtCl₂(PEt₃)L_B] and *cis*-[PtCl₂(PEt₃)L_C] to 11 and 12, respectively.

complex. (For the diazaphosphole complex **10** this assistance is lacking and dimerization does not occur.)

The dimerization then becomes complete by a similar interaction of N(=P) of the first molecule with either (i) the platinum atom of the second molecule together with another chloride shift—so affording symmetric **11** in a [3+3] addition—or (ii) the azaphosphole phosphorus atom of the second molecule—affording **12** in a [3+2] addition. A third feasible polynuclear structure would be an oligomeric complex based on P–N-connected azaphospholes, but such structures have, so far, only been verified in Cr(0) and W(0) pentacarbonyl derivatives.[3] Which of the first two alternatives is adopted is decided by two conflicting factors: Pt–N, P–Cl versus Pt–Cl, P–N bond energies on the one hand and ring size on the other. The species **7–9** stay monomeric since when X is Br the relative bond energies of Pt–X and P–X are less favorable to a halide shift than they are when X is Cl. Bearing in mind the dinuclear nature of the substrate and the intricate mechanism proposed, the bimolecular dimerization reaction discussed above is likely to be sensitive to steric influences. For both **11** and **12** only one set of NMR signals is seen and the involvement of a stereospecific pathway to the formation of single isomeric species seems likely.

Although in Figure 5 **11** is written as a complex of the bidentate (L_BCl) ligand in its phosphinoamide form (left resonance formula in Figure 6), it could also be viewed as a P,N-coordinated phosphazenide complex (employing the second resonance formula in Figure 6). The first representatives of the latter type of complex became known recently.[21]

Coordination Properties of Azaphosphole Ligands. Using the ³¹P NMR data of Table III, one can assess the coordination properties of the azaphospholes as N- and P-donors in the complexes studied. For example, the trans influence of L in *trans*-[MX₂(PR₃)L] can be estimated from either of the phosphorus parameters δ(P) (M = Pd)[14] and *J*(Pt,P) (M = Pt);[22] with increasing ligand influence δ(P) moves to higher field and *J*(Pt,P) decreases. The N-bound azaphospholes in **1–3** (M = Pd) and **4–6** (M = Pt) have, with use of data of [PtX₂(PEt₃)(py)][23] for comparison, a trans influence which is marginally less than that of pyridine and which decreases in the series py > L_C > L_A > L_B for both divalent metal centers. In the species **7–10**, where the azaphospholes are P-bound, *J*(Pt,P_L) is in all cases greater than 4.5 kHz, indicating a strong interaction with the Pt(II) center. The individual values of *J*(Pt,P_L), taken together with data for *cis*-[PtCl₂(PEt₃)(PPh₃)],[22b] indicate a P-donor ability for these azaphospholes which is clearly somewhat less than that of PPh₃ and which decreases in the order PPh₃ > L_B ≈ L_C > L_A. Unfortunately, data for the bromo analogue were not available, though the comparison remains valid since halide ions have a low trans influence and the change of X from bromine to chlorine in species of this type (e.g. **7** to **10**) has little effect on *J*(Pt,P_E) and leads to only a small increase in *J*(Pt,P_L). The *J*(Pt,P_E) values from the same complexes provide a similar order of PPh₃ > L_B > L_C > L_A for decreasing cis influence. These descriptions of the coordinating properties of the azaphosphole donor sites with Pd(II) and Pt(II) centers are complementary to previous results pertaining to zerovalent metal centers[3,5,6,8] and Au(III).[7]

It is also significant that it is the triazaphospholes L_B and L_C which do not form mononuclear species with [PtCl₂(PEt₃)]₂ and which produce, instead, the dinuclear products **11** and **12**.

Conclusions

In complexes of stoichiometry [MX₂(PEt₃)L] (M = Pt, Pd; X = Cl, Br; L = L_A, L_B, L_C) the metal and the anion present play important roles in determining whether σ-P or σ-N coordination of the azaphosphole occurs. With the diazaphosphole L_A only mononuclear species were identified, but with the triazaphospholes L_B and L_C possessing a P=N unit, further reaction to provide dinuclear species occurred when the metal was platinum and the halogen was chlorine.

(21) Susko, K. P. R.; Whittle, R. R.; Allcock, H. R. *J. Chem. Soc., Chem. Commun.* **1982**, 649.

(22) (a) Allen, F. H.; Pidcock, A.; Waterhouse, C. R. *J. Chem. Soc. A* **1970**, 2087. (b) Allen, F. H.; Sze, S. N. *J. Chem. Soc. A* **1971**, 2054.

(23) Hitchcock, P. B.; Jacobson, B.; Pidcock, A. *J. Chem. Soc., Dalton* **1977**, 2038–2042.